Supporting Information

Monoterpenoid Selenophenes Derived from (-)-Carvone with GPx-like activity

João P. Telo [a]*, Luis F. Veiros, [a] Vânia André,[a,b] João Ferreira da Silva, [a] Gonçalo C. Justino [a,c] and Alexandra M. M. Antunes [a]

a) Centro de Química Estrutural, Institute of Molecular Sciences, Departamento de Engenharia Química, Instituto Superior Técnico, Universidade de Lisboa, Av. Rovisco Pais, 1049-001 Lisboa, Portugal.

b) Associação do Instituto Superior Técnico para a Investigação e Desenvolvimento (IST-ID), Avenida António José de Almeida, 12, 1000-043 Lisboa, Portugal.

c) *Current adress*: Escola Superior de Tecnologia do Barreiro, Instituto Politécnico de Setúbal, Rua Américo da Silva Marinho, 2839-001 Barreiro, Portugal.

Table of Contents

1 General information 2
2 Theoretical calculations 2
2.1 Computational Details 2
2.2 Computed mechanism for the synthesis of 1 3
2.3 Computed mechanism for the synthesis of 6 8
3 Single crystal X-ray diffraction 8
4 NMR and mass spectra 11
4.1 Mentoselenophenone 1 11
4.2 Phenol 2 12
4.3 Phenol 3 13
4.4 Compound 4 14
4.5 Compound 5 15
4.6 Dimer 6 16
4.7 Oxime 7 17
4.8 Lactam 8 18

1 General information

Column flash chromatography was done using 60 Å 70-200 μ silica gel dried at 200º C under vacuum and kept under nitrogen. Analytical thin layer chromatography (TLC) was carried out on silica gel plates (Silica Gel 60 F with fluorescent indicator 254 nm). ^{1}H, ^{13}C, COSY, HMQC and HMBC NMR spectra were recorded on a Bruker 400 MHz Advance II NMR spectrometer. Chemical shifts (δ scale) are reported in parts per million (ppm) relative to the central peak of the solvent. Melting points were determined on capillary and are uncorrected. HRMS analysis was performed using a Orbitrap Exploris Mass Spectrometer.

2 Theoretical calculations

2.1 Computational Details

Calculations were performed using the Gaussian 09 software package[S1] and the PBE0 functional, without symmetry constraints. That functional uses a hybrid generalized gradient approximation (GGA), including 25 % mixture of Hartree-Fock[S2] exchange with DFT[S3] exchange-correlation, given by Perdew, Burke and Ernzerhof functional (PBE).[S4] The model used for the calculations included one extra Br_2 molecule that stabilized the bromide ion loss in the form of Br_3^-, in the first step of the mechanism. The optimized geometries were obtained with a standard 6-31+G(d,p).[S5] Transition state optimizations were performed with the Synchronous Transit-Guided Quasi-Newton Method (STQN) developed by Schlegel *et al*,[S6] following extensive searches of the Potential Energy Surface. Frequency calculations were performed to confirm the nature of the stationary points, yielding one imaginary frequency for the transition states and none for the minima. Each transition state was further confirmed by following its vibrational mode downhill on both sides and obtaining the minima presented on the energy profile. The electronic energies (E_{b1}) obtained at the PBE0/6-31+G(d,p) level of theory were converted to free energy at 298.15 K and 1 atm (G_{b1}) by using zero point energy and thermal energy corrections based on structural and vibration frequency data calculated at the same level.

Solvent effects (CH_2Cl_2 in the formation of **1** and THF in the formation of **6**) were accounted for in all calculations (including geometry optimizations) by means of the Polarisable Continuum Model (PCM) initially devised by Tomasi and coworkers[S7] with radii and non-electrostatic terms of the SMD solvation model, developed by Truhler et al.[S8] Single point energy calculations were performed on the geometries obtained at the PBE0/6-31+G(d,p) level using the same functional and a 6-311++G(d,p) basis set.[S9] The free energy values presented (G_{b2}-D3) were corrected for dispersion by means of Grimme DFT-D3 method[S10] with Becke and Johnson short distance damping,[S11] being derived from the electronic energy values obtained at the PBE0-D3/6-311++G(d,p)//PBE0/6-31+G(d,p) level (E_{b2}-D3) according to the following expression:

$(G_{b2}\text{-D3}) = (E_{b2}\text{-D3}) + G_{b1} - E_{b1}$

2.2 Computed mechanism for the synthesis of 1

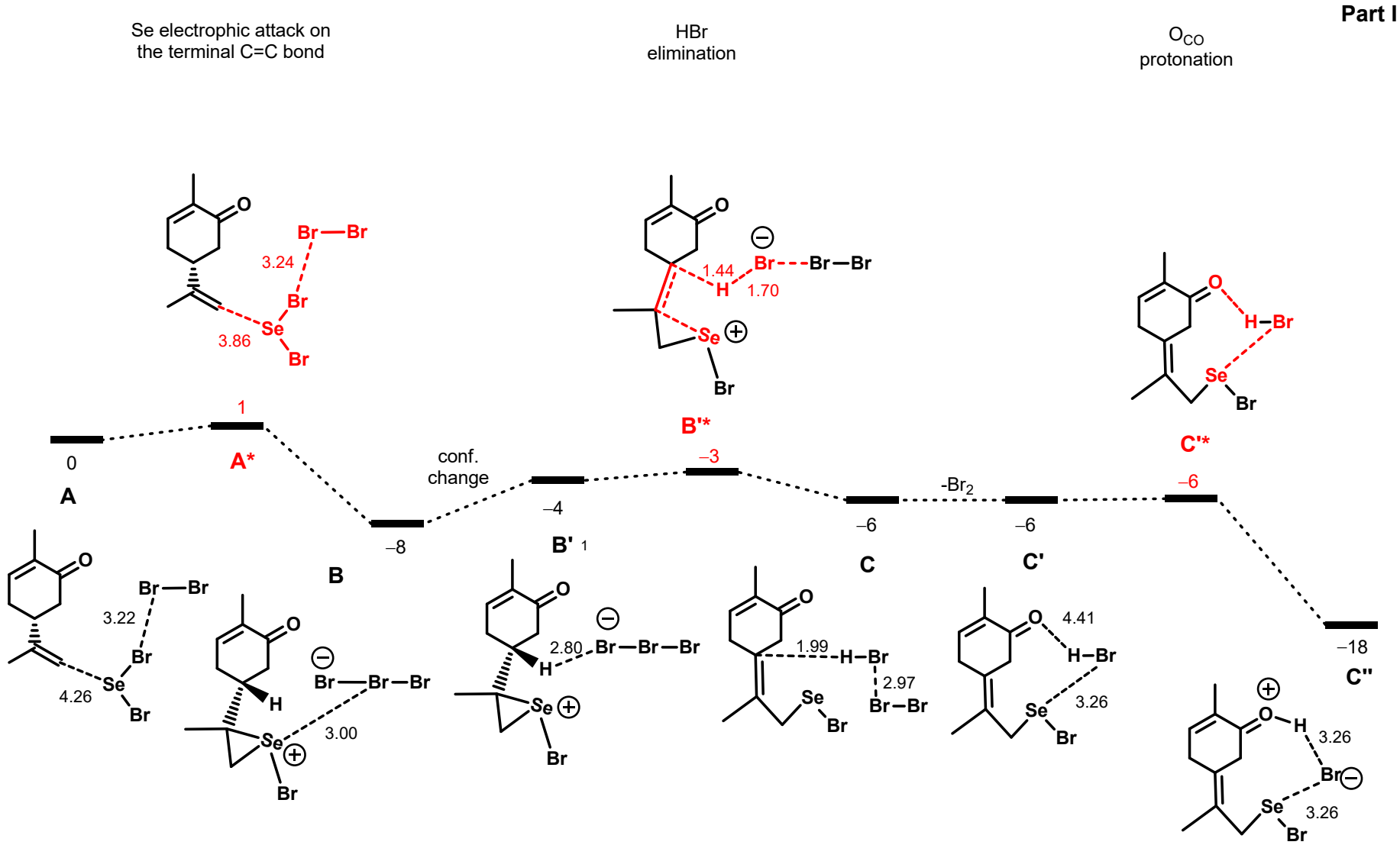

Figure S1. Free energy profile for the formation of **1** from (-)-Carvone (Part I). Distances in Å and free energy values (kcal/mol) relative to **A** (**A** is 14 kcal/mol less stable then the separated reactants: (-)-Carvone + $SeBr_2$ + Br_2).

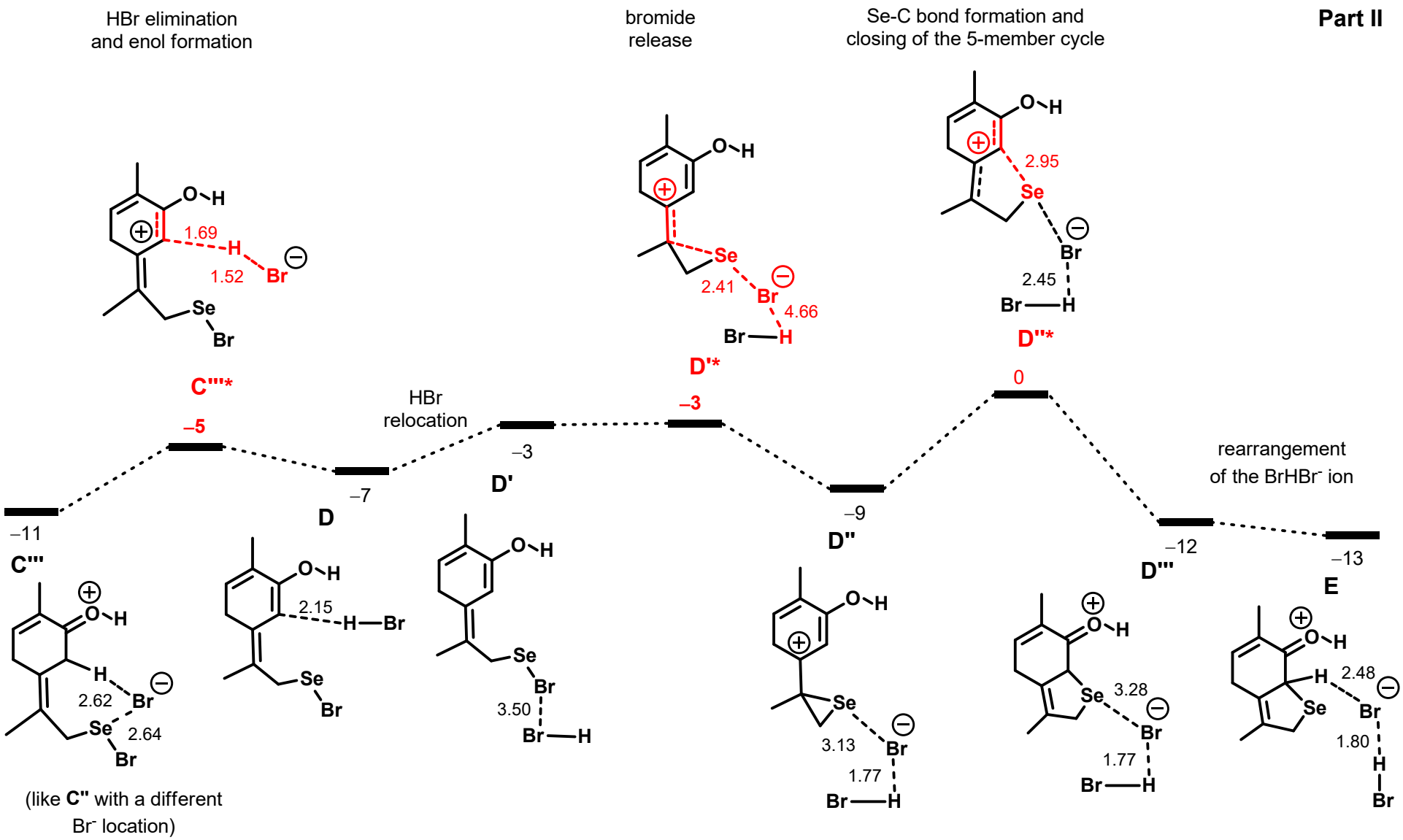

Figure S2. Free energy profile for the formation of **1** from (-)-Carvone (Part II). Distances in Å and free energy values (kcal/mol) relative to **A**.

Part III

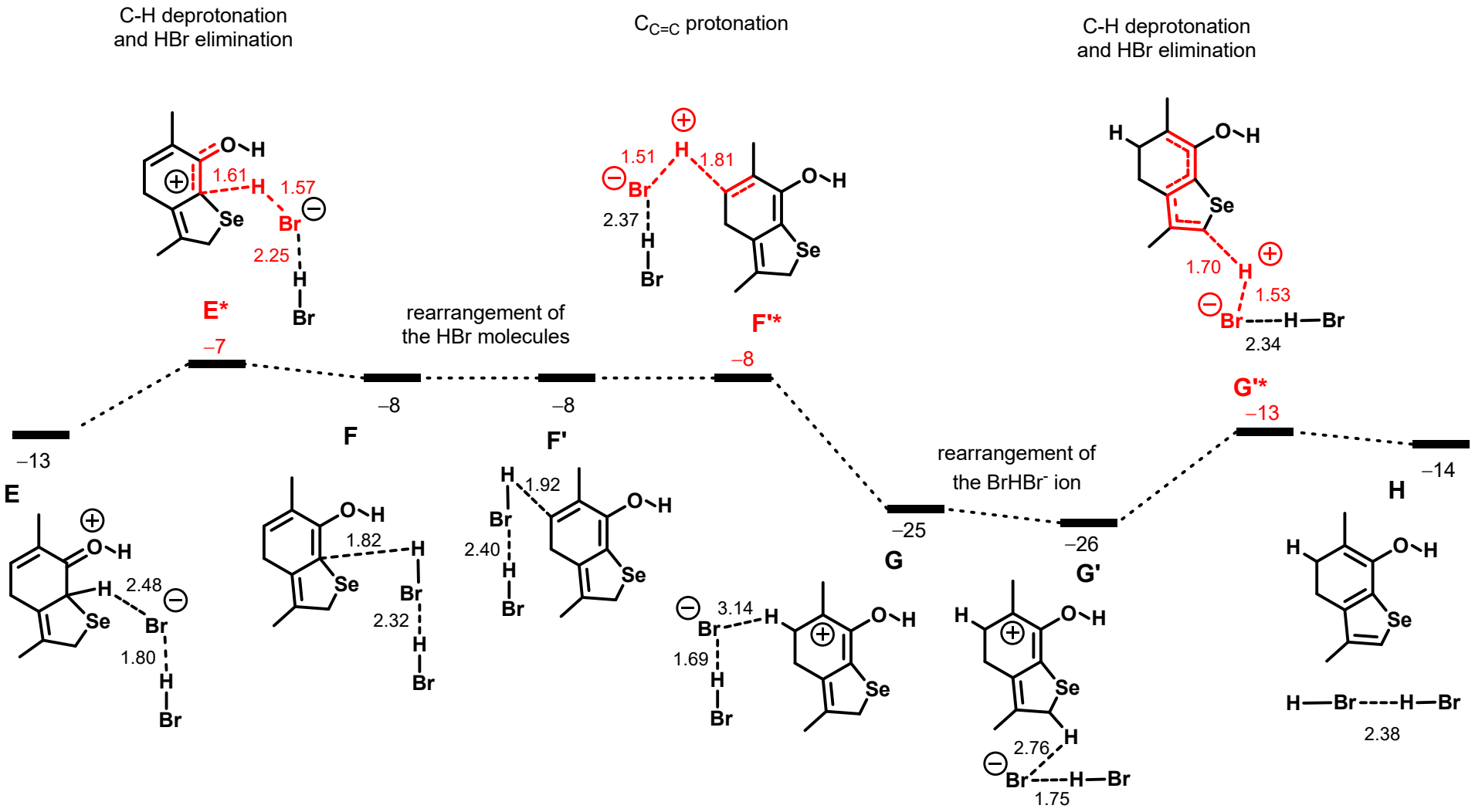

Figure S3. Free energy profile for the formation of **1** from (-)-Carvone (Part III). Distances in Å and free energy values (kcal/mol) relative to **A**.

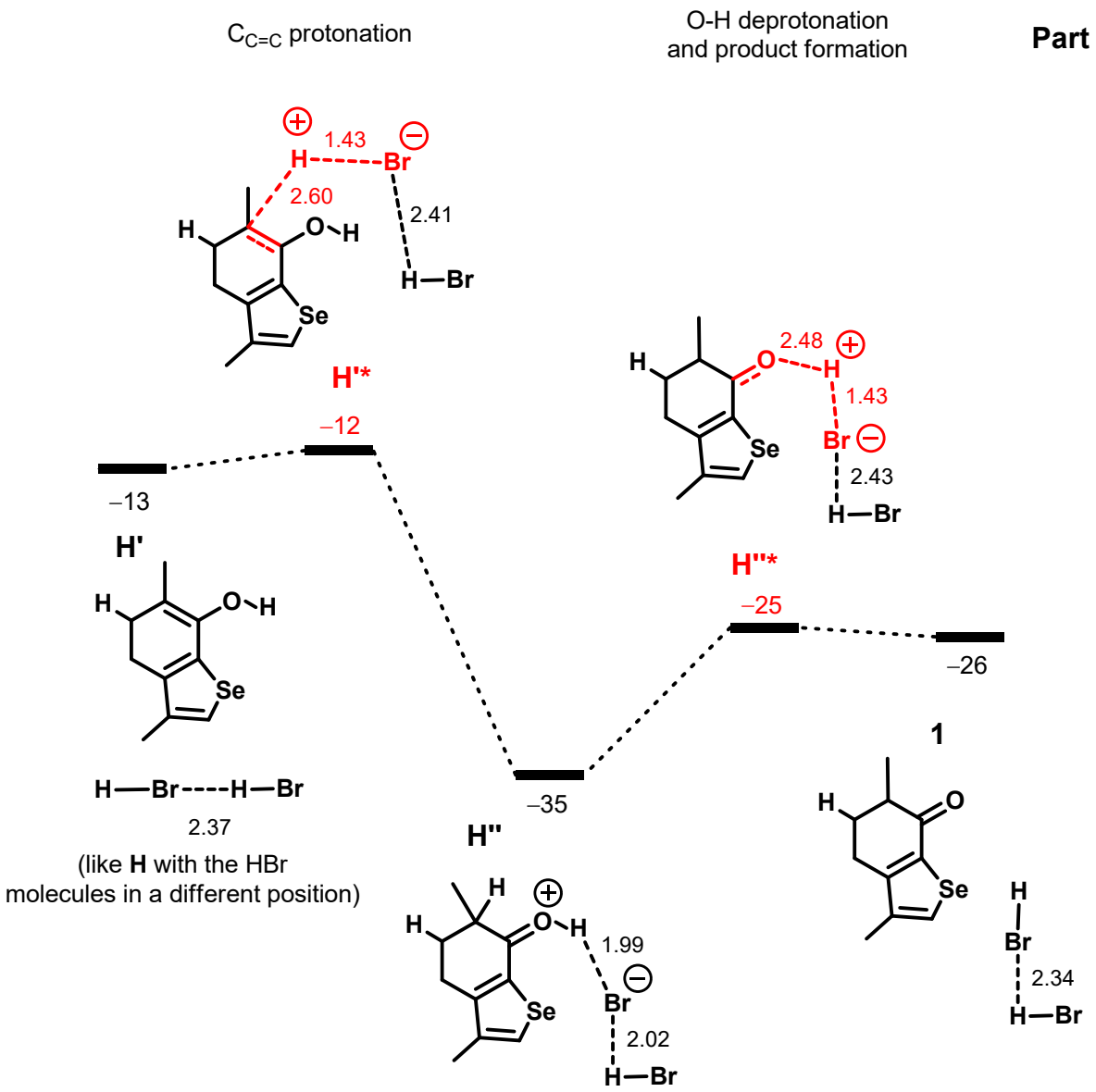

Figure S4. Free energy profile for the formation of **1** from (-)-Carvone (Part IV). Distances in Å and free energy values (kcal/mol) relative to **A**.

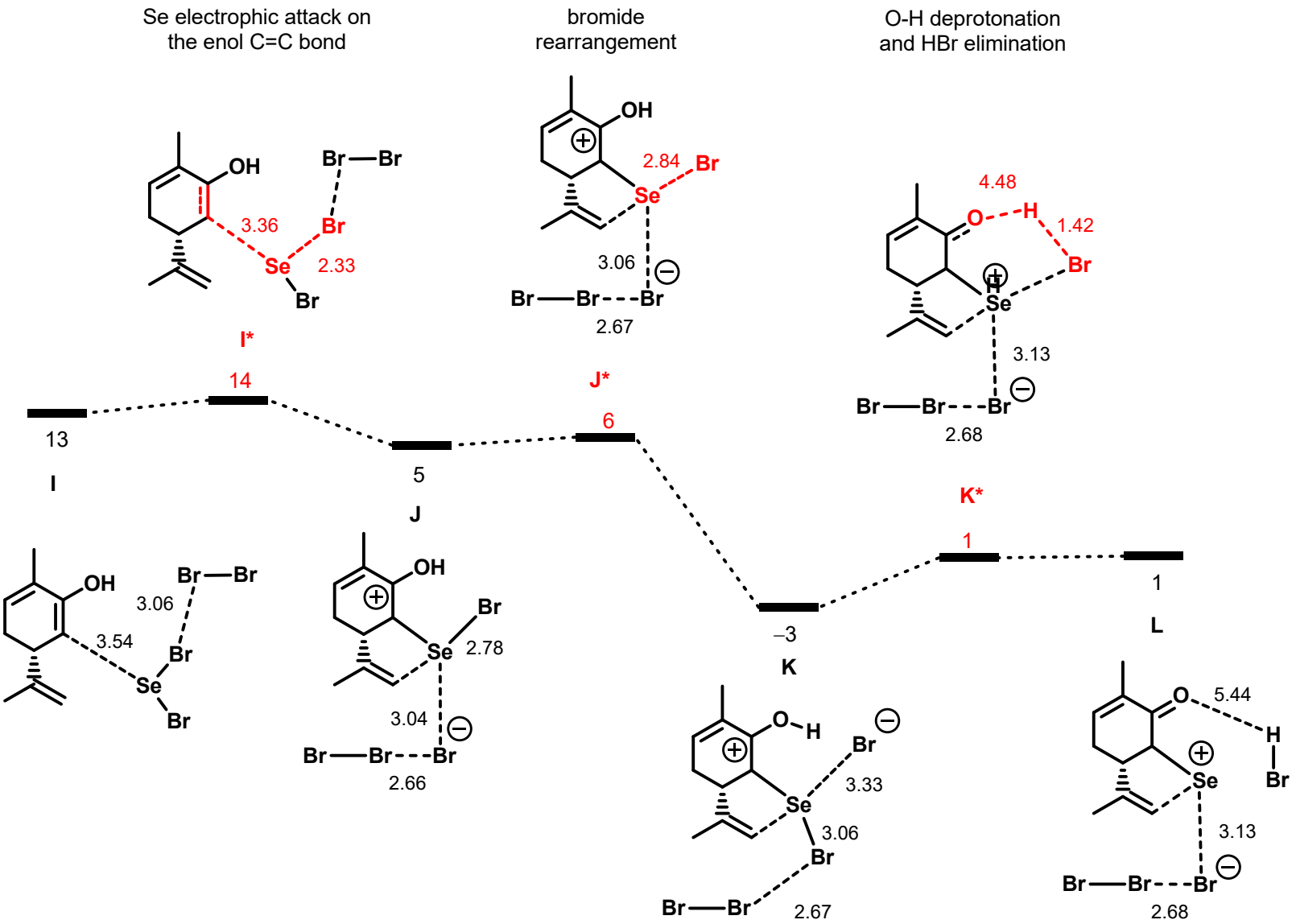

Figure S5. Free energy profile for $SeBr_2$ electrophilic attack on the C=C double bond of the carvone enol. Distances in Å and free energy values (kcal/mol) relative to **A**.

2.3 Computed mechanism for the synthesis of 6

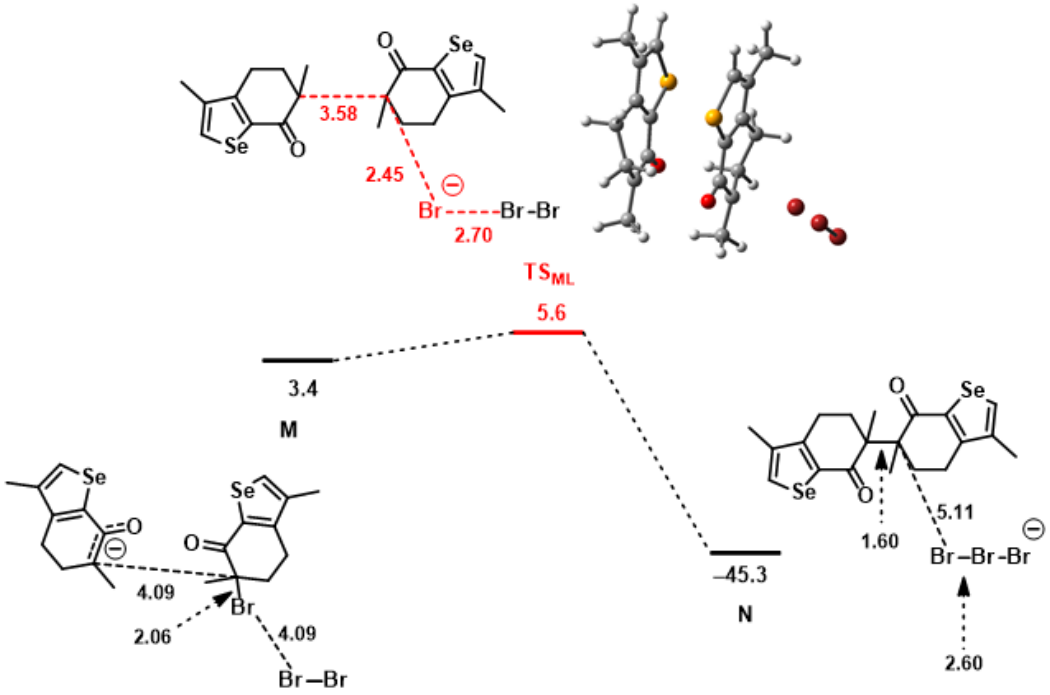

Figure S6. Free energy profile for the formation of **6** from the enolate of **1** and product **4** (assisted by a Br_2 molecule). Distances in Å and free energy values (kcal/mol) relative to the separated reactants (enolate + **4** + Br_2).

3 Single crystal X-ray diffraction

X-ray crystallographic data for compounds **1**, **2** and **6** were collected from single crystals using an area detector diffractometer (Bruker AXS-KAPPA APEX II) at room temperature and graphite-monochromated Mo Kα (λ = 0.71073 Å) radiation. Cell parameters were retrieved using Bruker APEX2[S12] software and refined with Bruker SAINT[S13] on all observed reflections. Absorption corrections were applied using SADABS.[S14] The structures were solved by direct methods using SHELXT[S15] and refined with full-matrix least-squares refinement against F^2 using SHELXL-2014/7.[S13] These two programs are included in the WINGX-Version 2021.33 program package.[S16] All non-hydrogen atoms were refined anisotropically, and the hydrogen atoms were inserted in idealized positions, riding on the parent C atom. Drawings were made using Mercury 2024.2.0 and Olex^2 – 1.2.7,[S17,S18] a program that was also used to calculate Ring planarity. Relevant details of the X-ray data analysis are displayed in **Table S1**. Crystallographic data for compounds **1**, **4** and **6** was deposited with the Cambridge Crystallographic Data Centre (CCDC 2394794-2394796) and can be obtained free of charge from: CCDC, 12 Union Road, Cambridge CB2 1EZ, UK (Fax: 44-1223-226033; e-mail: deposit@ccdc.cam.ac.uk) or http://www.ccdc.cam.ac.uk/deposit.

Table S1. Crystallographic details for compounds **1**, **4** and **6**.

	1	**4**	**6**
Chemical formula	$C_{10}H_{12}OSe$	$C_{10}H_{11}BrOSe$	$C_{20}H_{22}O_2Se_2$
Formula weight	227.16	306.05	453.29
Crystal colour	Colourless	Colourless	Colourless
Crystal size (mm)	0.18 x 0.10 x 0.04	0.20 x 0.15 x 0.15	0.18 x 0.12 x 0.06
Crystal system	Monoclinic		Triclinic
Space group	$P2_1/n$	$P2_1/n$	P-1
a (Å)	7.300(7)	7.767(3)	10.0831(14)
b (Å)	10.3528(9)	10.906(4)	10.4303(15)
c (Å)	12.964(12)	12.122(4)	10.7237(16)
α (°)	90	90	71.641(6)
β (°)	91.02	90.882)	70.303(6)
γ (°)	90	90	63.501(6)
V (Å^3)	980.1(15)	1026.7(6)	932.0(2)
Z	4	4	2
d (mg.cm^{-3})	1.539	1.980	1.612
μ (mm^{-1})	3.781	7.506	3.976
θ range (°)	2.517-25.319	3.095-25.680	2.225-25.745
Reflections collected/unique	10862/1789	6465/1949	24783/3552
R_{int}	0.1127	0.033	0.1552
GoF	1.019	1.022	1.012
Final R indices[a,b] [$I > 2\sigma(I)$]	R_1=0.0650, wR_2 =0.1539	R_1=0.0376, wR_2 =0.0827	R_1=0.0561, wR_2 =0.0915

[a] $R_1 = \Sigma||F_o| - |F_c||/\Sigma|F_o|$; [b] $wR_2 = [\Sigma[w(F_o^2 - F_c^2)^2]/\Sigma[w(F_o^2)^2]]^{1/2}$

Table S2. Root-mean-square deviation of plane S1-C2-C3-C3A-C7A and individual atom deviations for compounds **1**, **4** and **6**.

		1	**4**	**6**	
RMSD[a] deviation [Å]		**0.00405**	**0.007987**	**0.010227**	**0.002757**
Average atom deviation from plane S1-C2-C3-C3A-C7A (Å)		0.0036	0.007	0.009	0.0024
Atom absolute deviation from plane S1-C2-C3-C3A-C7A (Å)	Se1 (Se2)	0.002	0.005	0.002	0.003
	C2 (C10)	0.005	0.001	0.005	0.002
	C3 (C11)	0.006	0.007	0.013	0.000
	C3A (C11A)	0.004	0.012	0.015	0.003
	C7A (C15A)	0.001	0.01	0.01	0.004

a – Root-mean-square deviation

Table S3 – Bond lengths for compounds 1, 4 and 6

Bond	Bond length / Å		
	1	4	6
C(2)-C(3)	1.346(13)	1.355(7)	1.359(8)
C(2)-Se(1)	1.849(10)	1.847(5)	1.856(7)
C(3)-C(3A)	1.425(12)	1.423(6)	1.422(8)
C(3)-C(8)	1.515(13)	1.494(7)	1.500(9)
C(3A)-C(7A)	1.361(11)	1.360(6)	1.367(8)
C(3A)-C(4)	1.513(12)	1.490(6)	1.505(8)
C(4)-C(5)	1.465(13)	1.518(6)	1.510(8)
C(5)-C(6)	1.353(11)	1.512(6)	1.529(7)
C(6)-C(7)	1.485(13)	1.526(7)	1.531(7)
C(6)-C(9)	1.558(14)	1.561(6)	1.557(7)
C(7)-O(1)	1.214(12)	1.208(6)	1.234(6)
C(7)-C(7A)	1.453(15)	1.447(6)	1.465(8)
C(7A)-Se(1)	1.874(8)	1.860(5)	1.860(5)
Br(1)-C(6)	n/A	1.991(4)	n/A
Se(2)-C(10)	n/A	n/A	1.852(7)
Se(2)-C(15A)	n/A	n/A	1.874(5)
O(2)-C(15)	n/A	n/A	1.216(7)
C(15)-C(15A)	n/A	n/A	1.445(8)
C(15)-C(14)	n/A	n/A	1.546(7)
C(6)-C(14)	n/A	n/A	1.577(8)
C(14)-C(17)	n/A	n/A	1.546(7)
C(14)-C(13)	n/A	n/A	1.549(8)
C(15A)-C(11A)	n/A	n/A	1.362(8)
C(11A)-C(11)	n/A	n/A	1.441(8)
C(11A)-C(12)	n/A	n/A	1.494(8)
C(11)-C(10)	n/A	n/A	1.342(8)
C(11)-C(16)	n/A	n/A	1.510(9)
C(12)-C(13)	n/A	n/A	1.516(8)

4 NMR and mass spectra

4.1 Mentoselenophenone 1

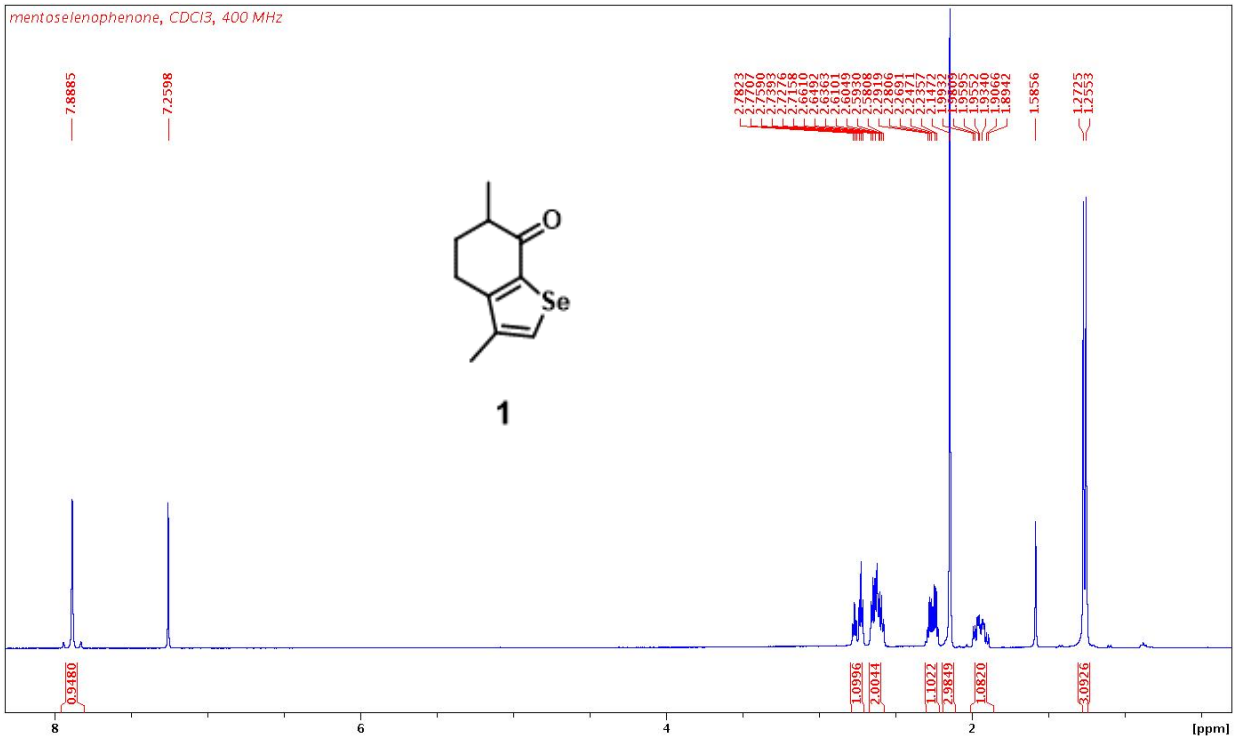

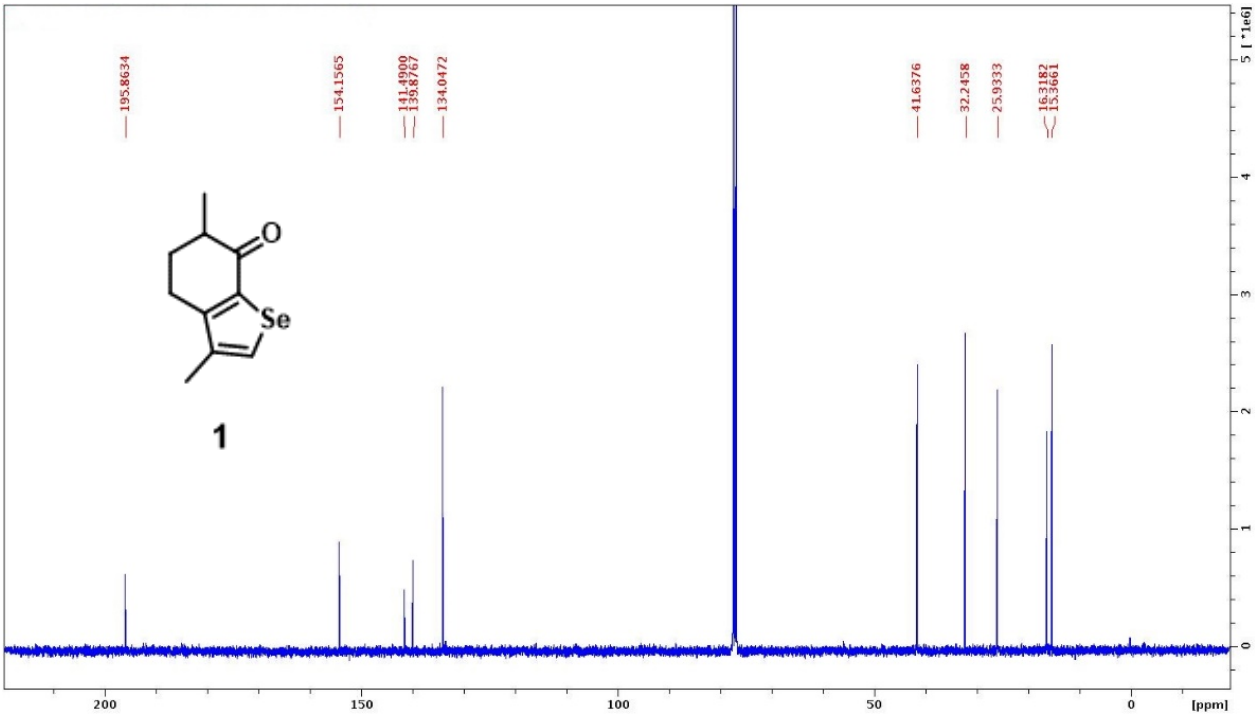

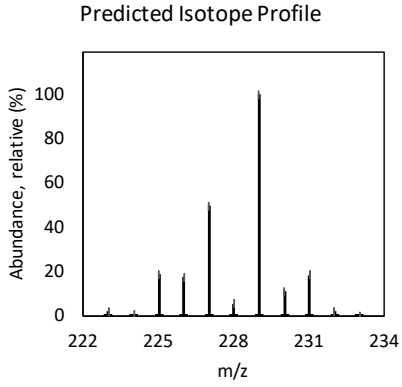

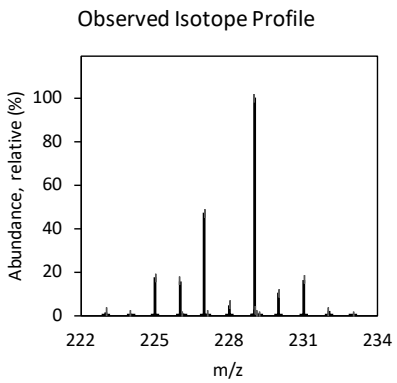

4.2 Phenol 2

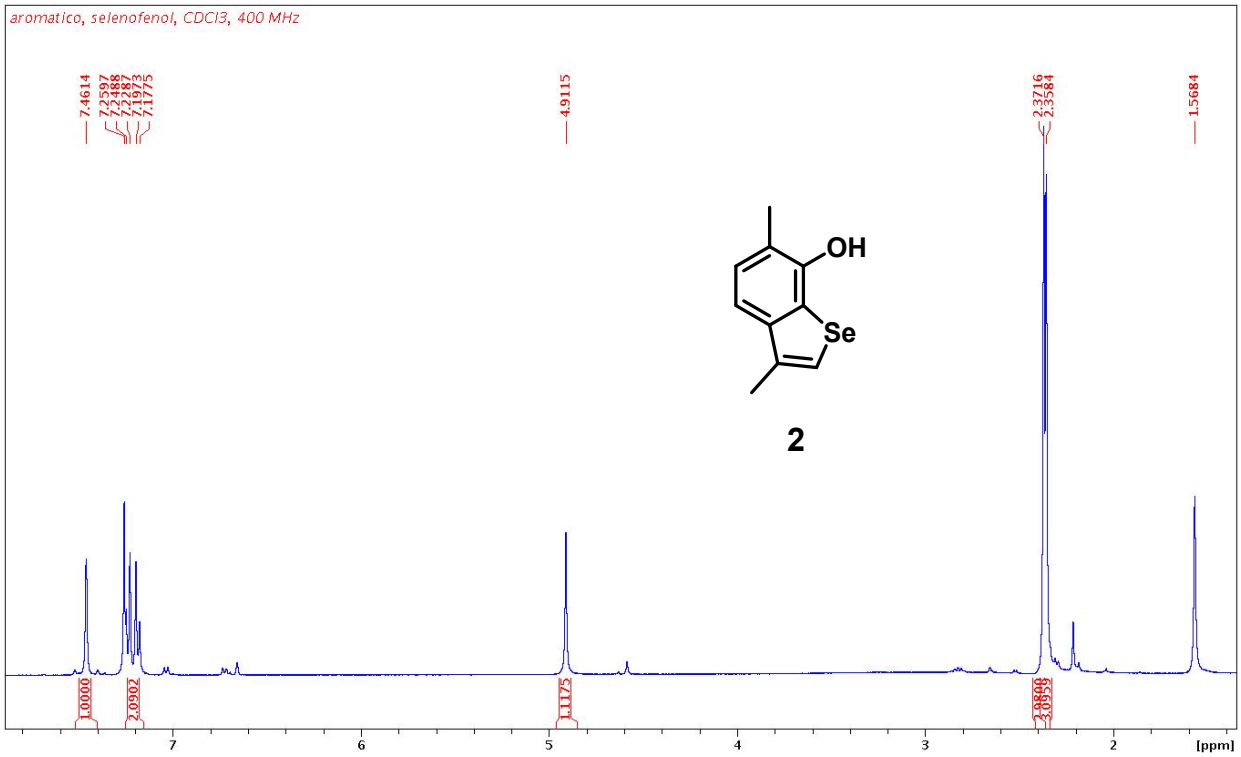

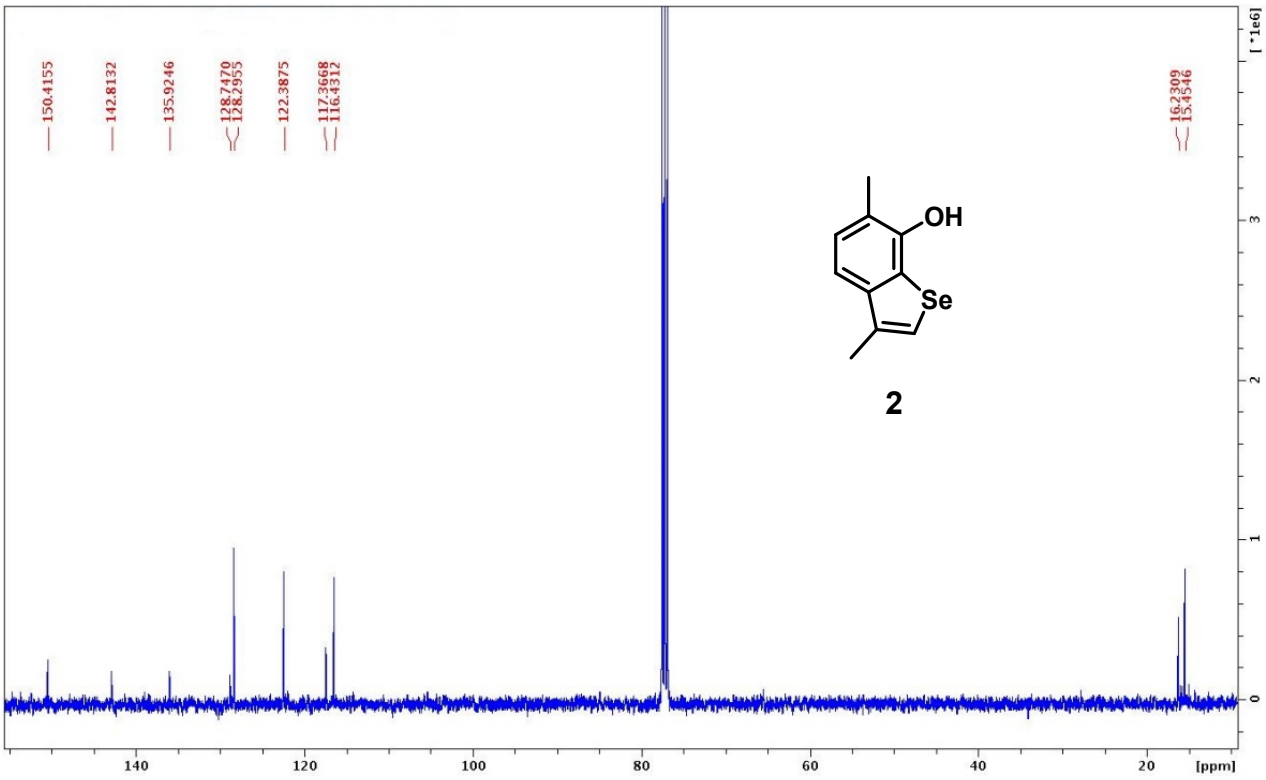

Predicted Isotope Profile

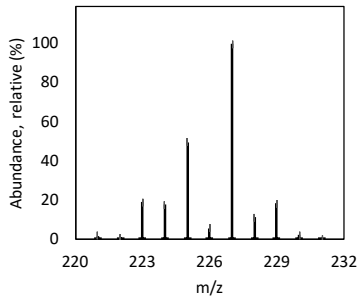

Observed Isotope Profile

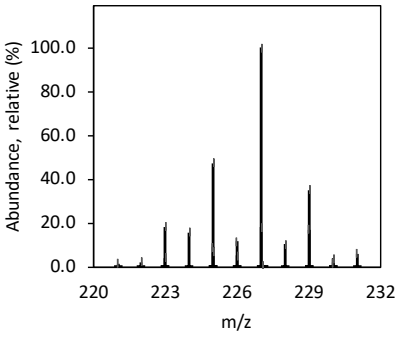

4.3 Phenol 3

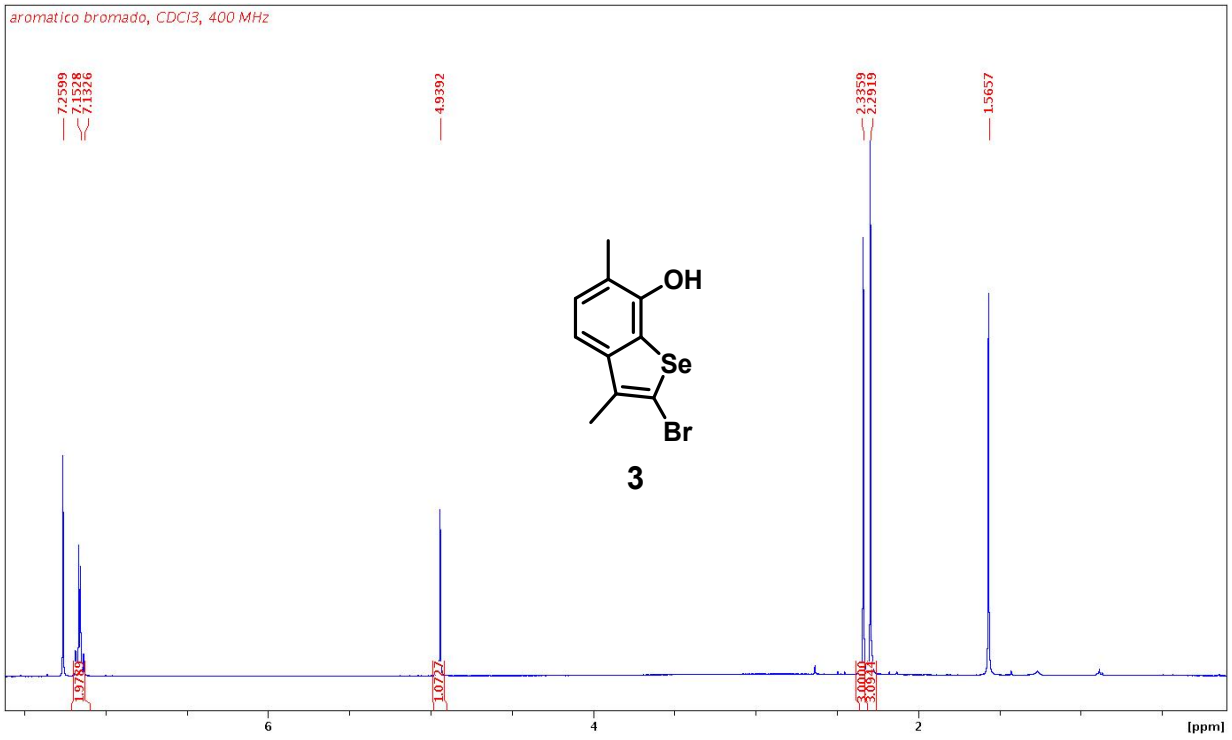
aromatico bromado, CDCl3, 400 MHz
7.2599
7.1528
7.1326
4.9392
2.3359
2.2919
1.5657
OH
Se
Br
3
1.9780
1.0727
3.0000
3.0921
6
4
2
[ppm]

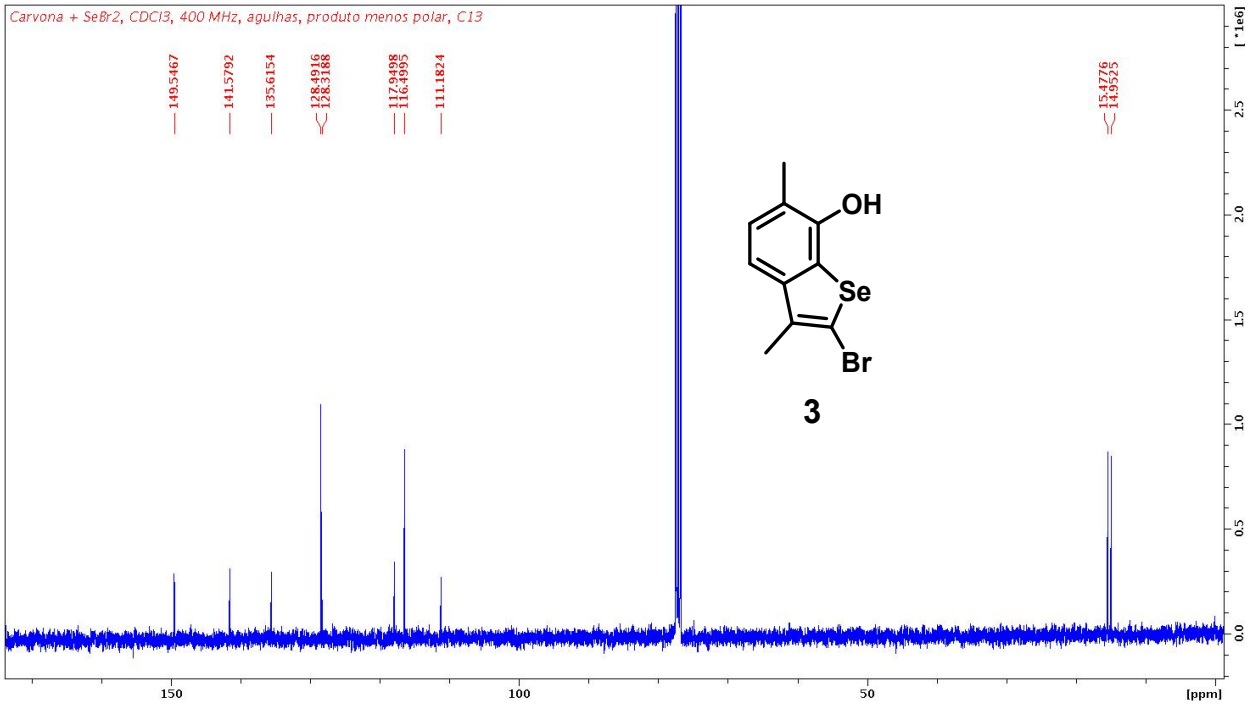
Carvona + SeBr2, CDCl3, 400 MHz, agulhas, produto menos polar, C13
149.5467
141.5792
135.6154
128.4916
128.3188
117.9498
116.4995
111.1824
15.4776
14.9525
OH
Se
Br
3
[*1e6]
150
100
50
[ppm]

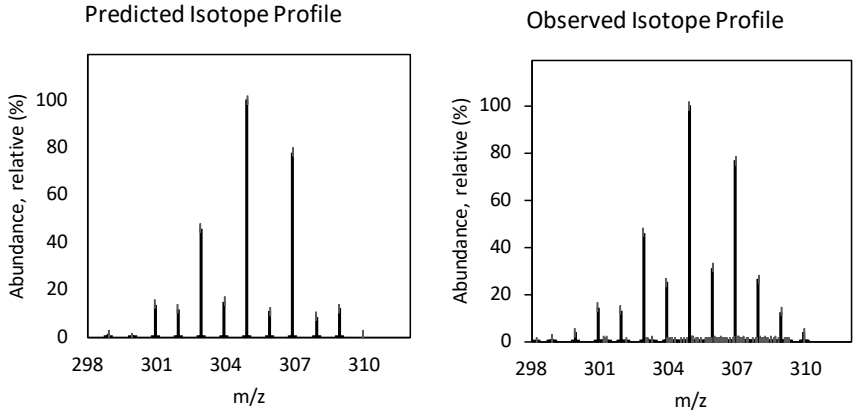
Predicted Isotope Profile
Abundance, relative (%)
100
80
60
40
20
0
298
301
304
307
310
m/z
Observed Isotope Profile
Abundance, relative (%)
100
80
60
40
20
0
298
301
304
307
310
m/z

4.4 Compound 4

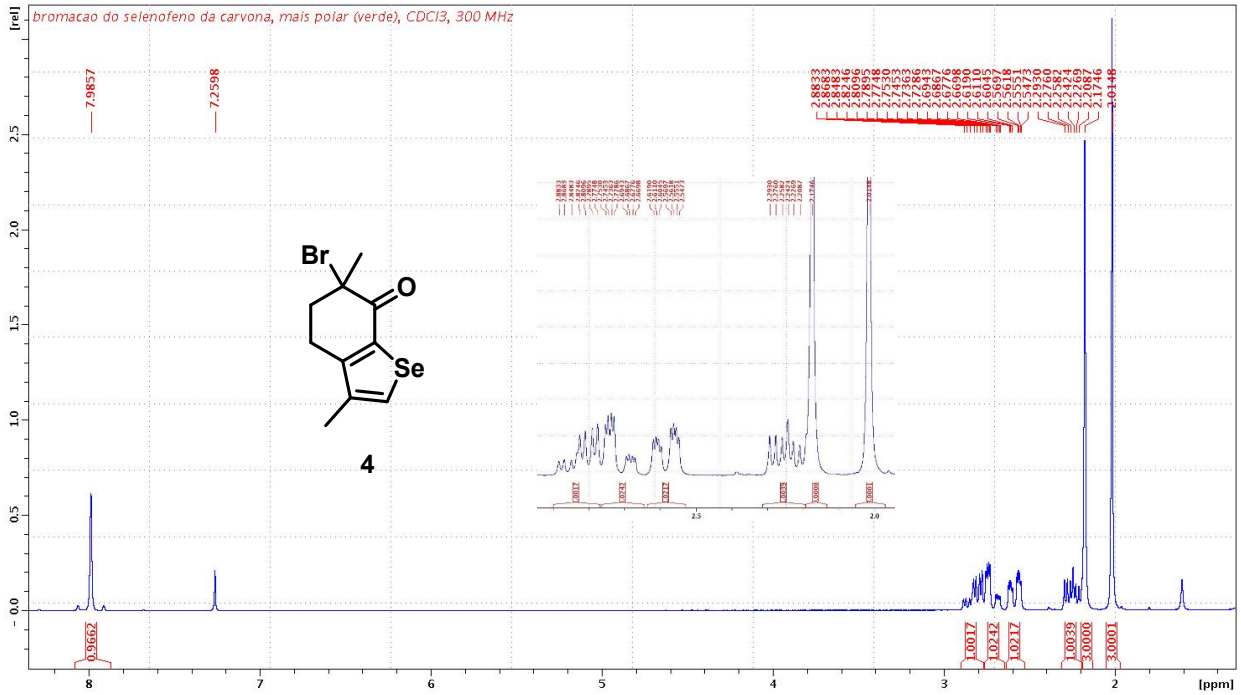

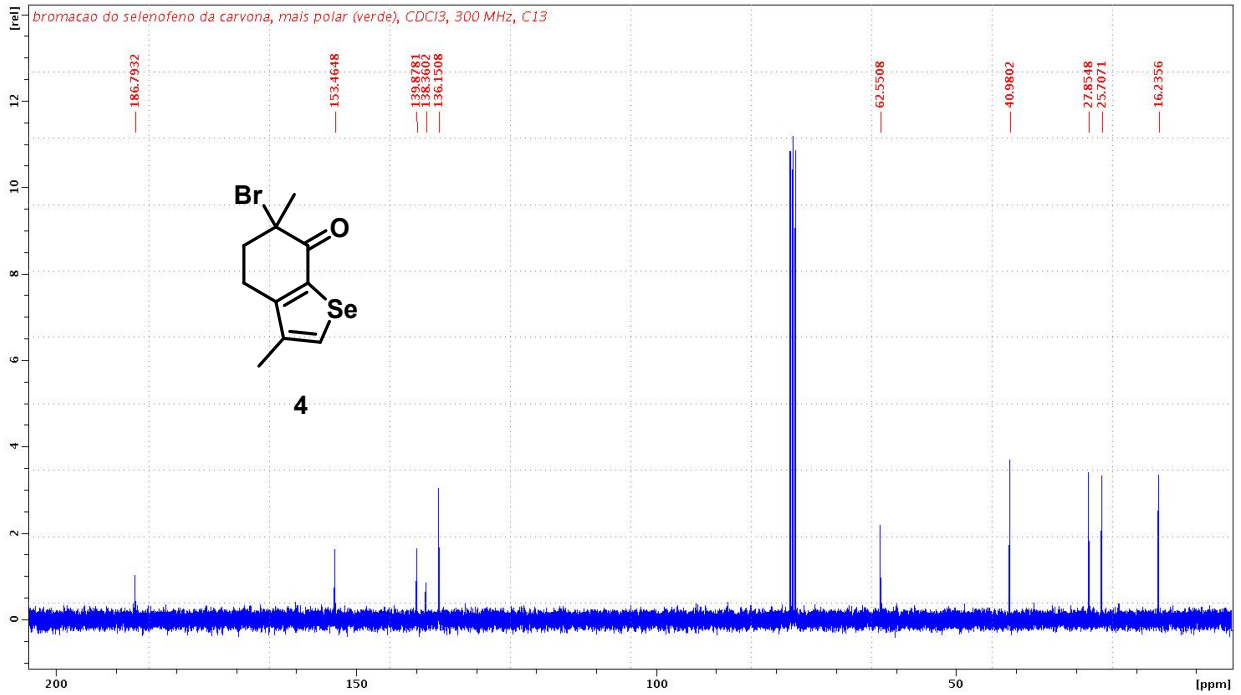

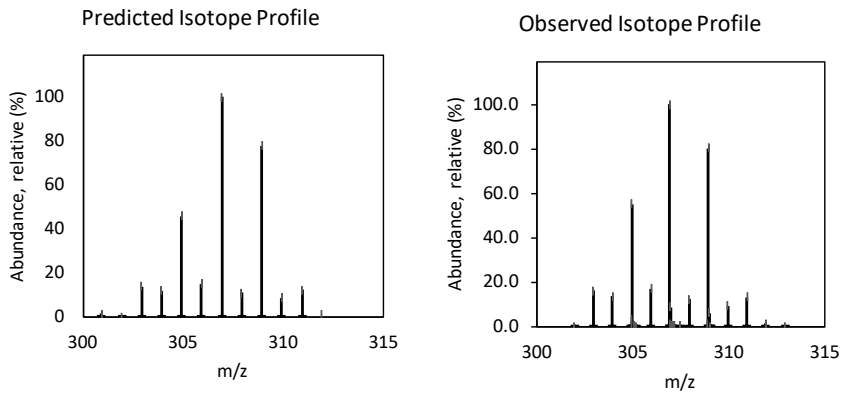

4.5 Compound 5

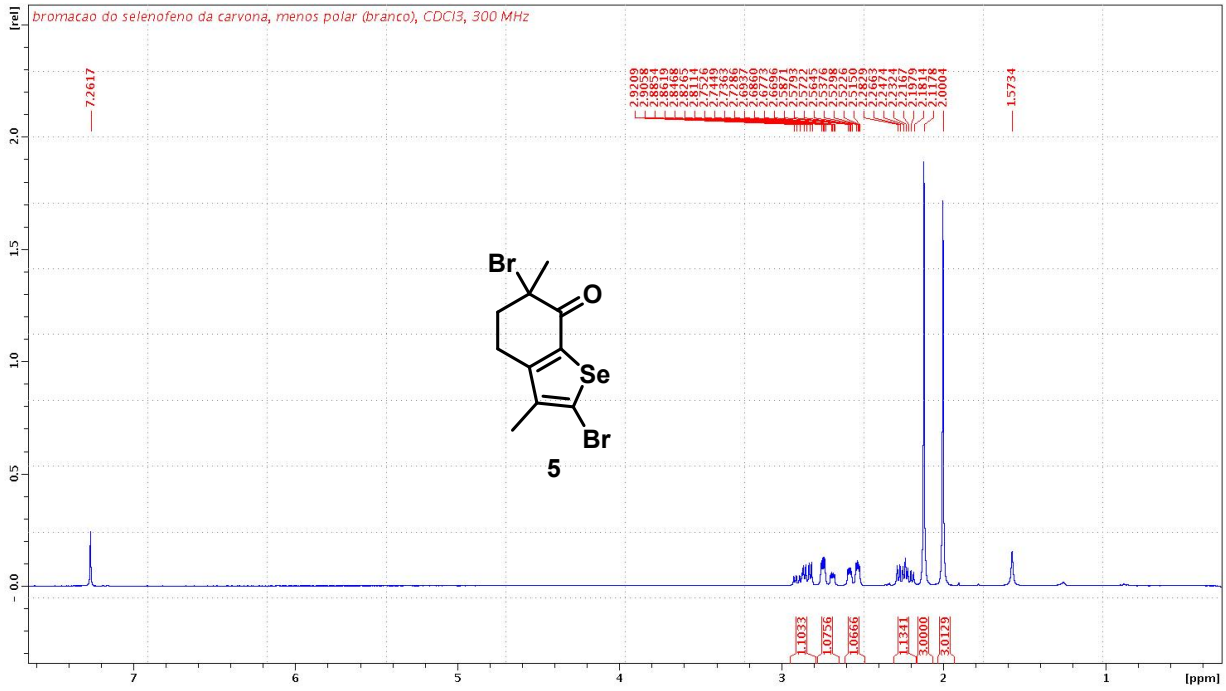

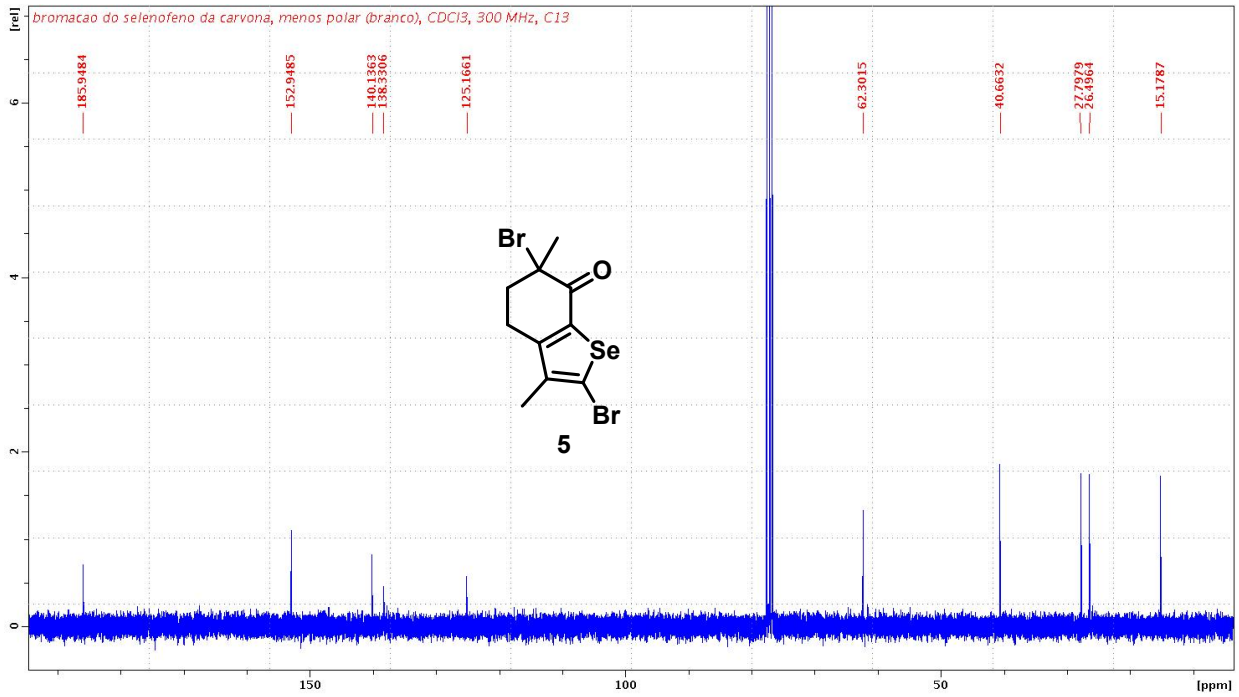

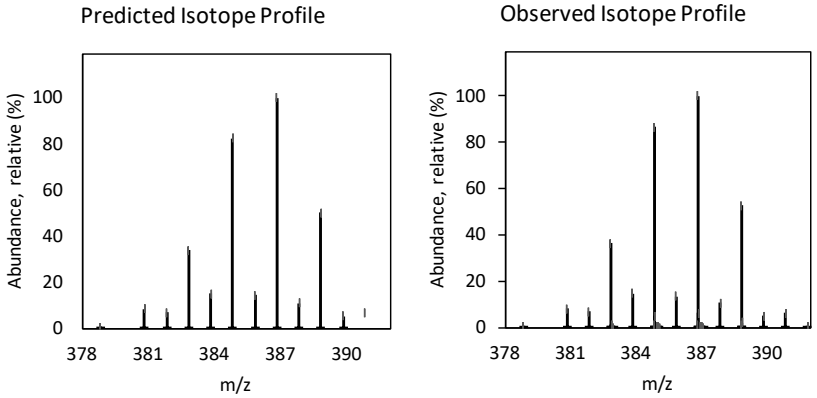

4.6 Dimer 6

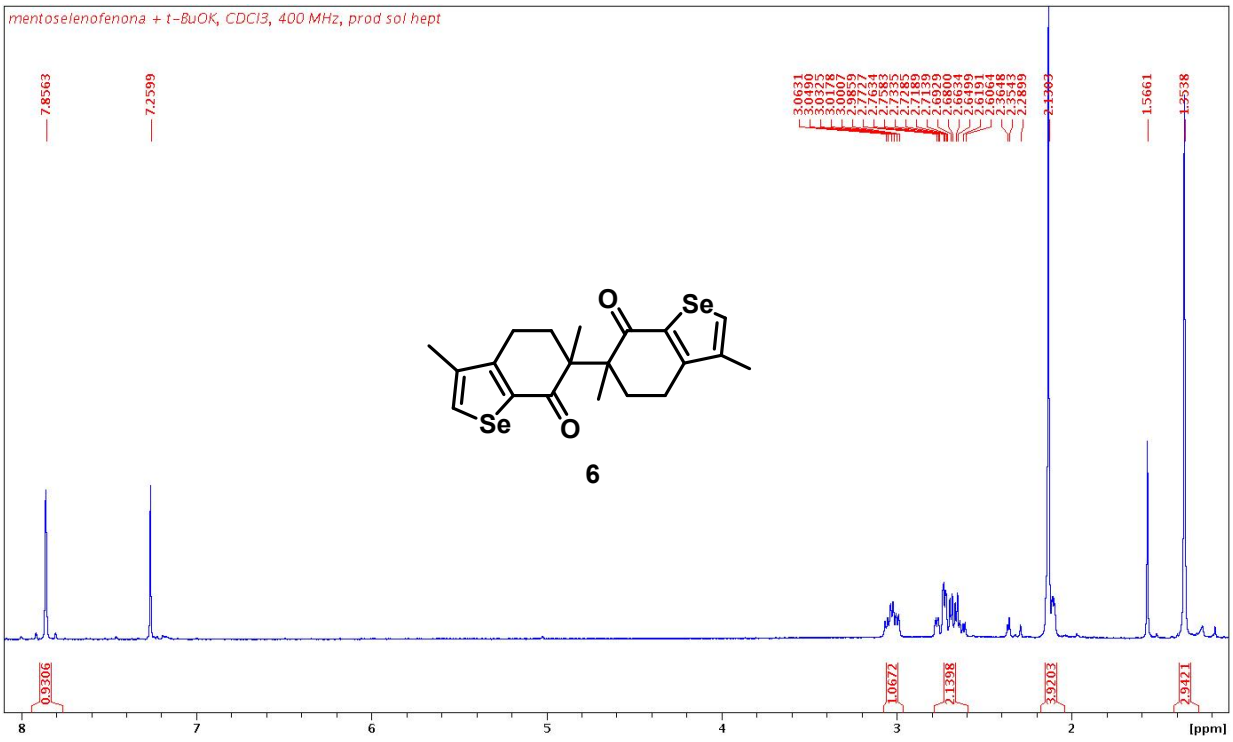
mentoselenofenona + t-BuOK, CDCl3, 400 MHz, prod sol hept
7.8563
7.2599
1.5661
1.3538
0.9306
1.0672
2.1398
3.9203
2.9421
[ppm]
6

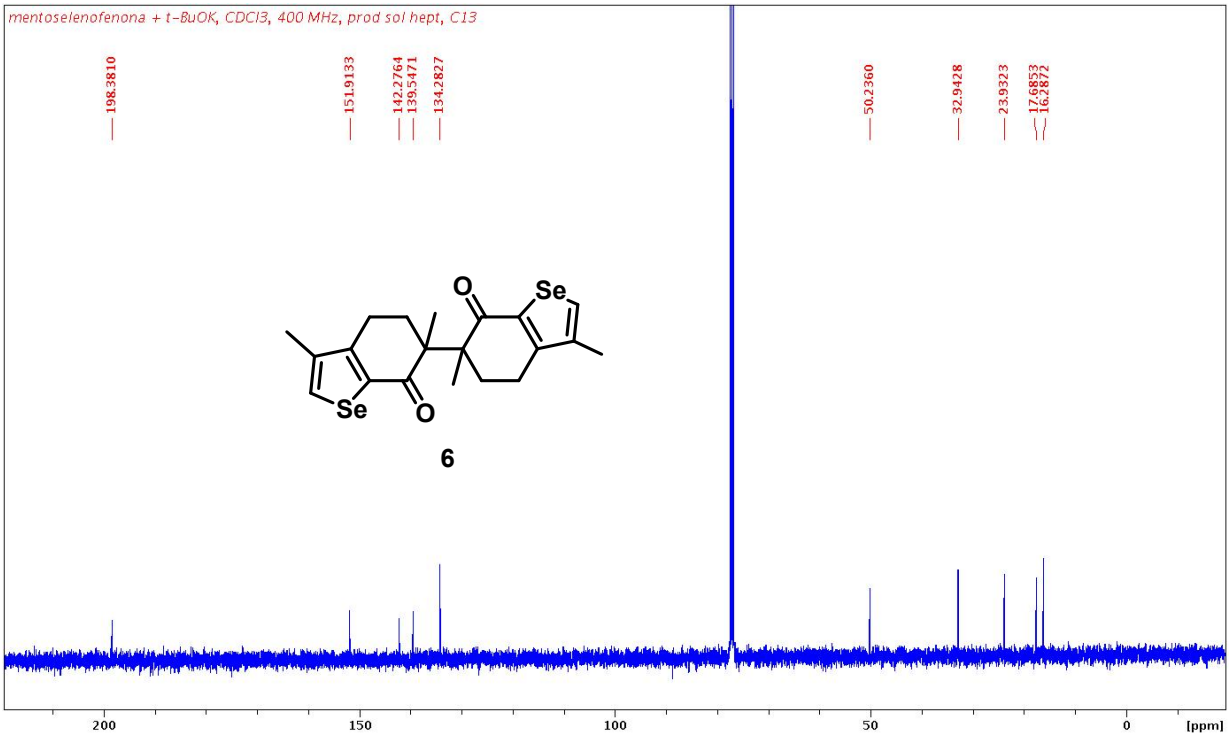
mentoselenofenona + t-BuOK, CDCl3, 400 MHz, prod sol hept, C13
198.3810
151.9133
142.2764
139.5471
134.2827
50.2360
32.9428
23.9323
17.6853
16.2872
[ppm]
6

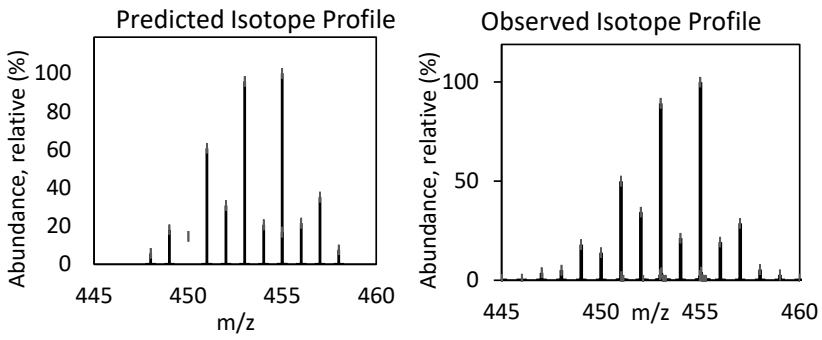
Predicted Isotope Profile
Abundance, relative (%)
m/z
Observed Isotope Profile
Abundance, relative (%)
m/z

4.7 Oxime 7

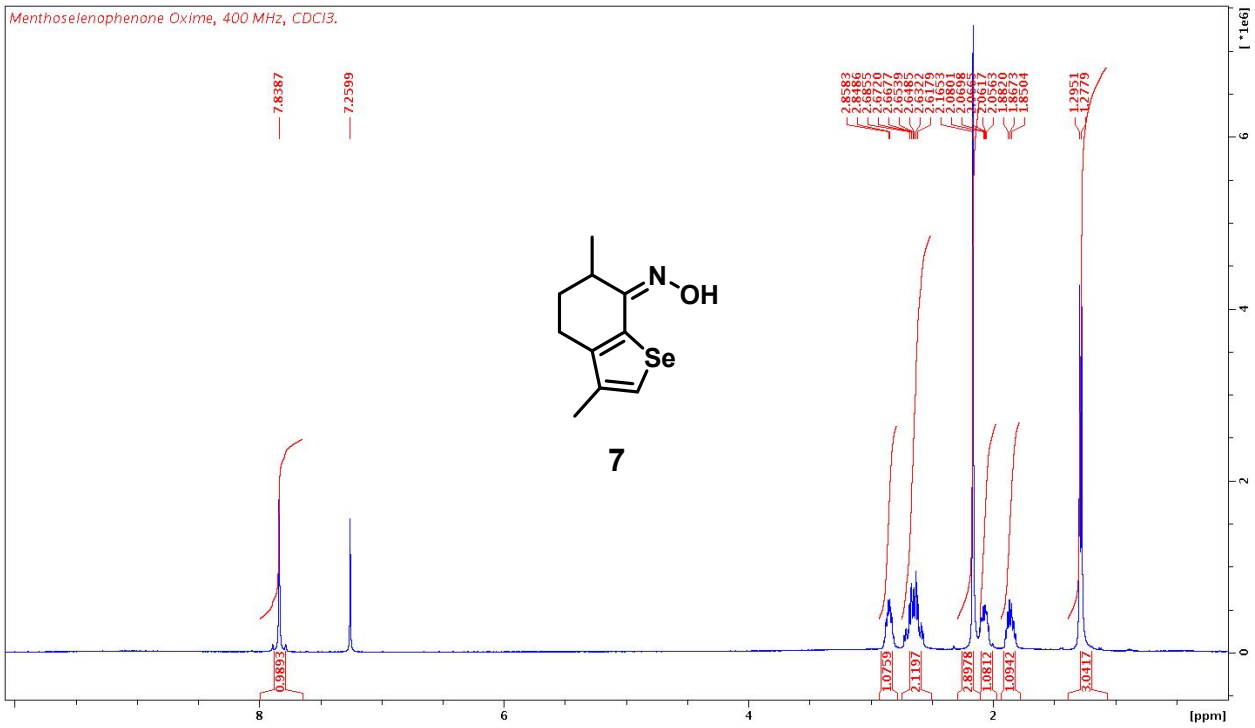
Menthoselenophenone Oxime, 400 MHz, CDCl3.
7.8387
7.2599
1.2951
1.2779
0.9893
1.0759
2.1197
2.8978
1.0812
1.0942
3.0417
[*1e6]
[ppm]
N
OH
Se
7

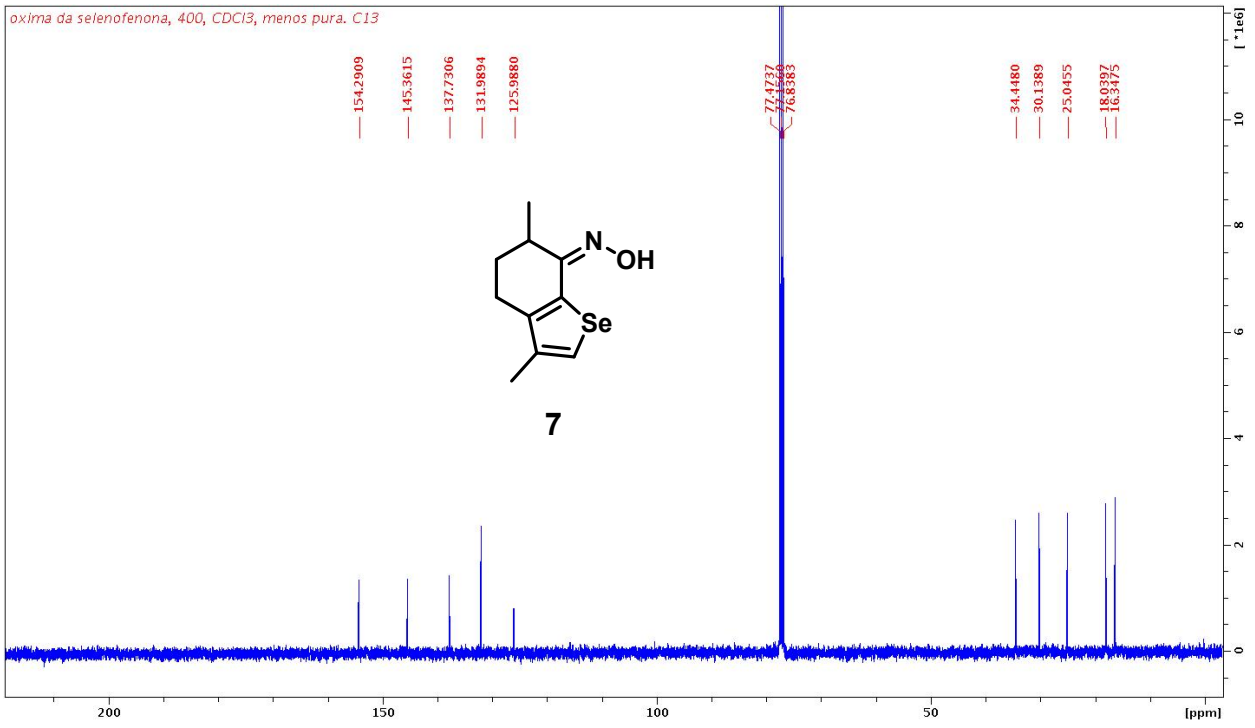
oxima da selenofenona, 400, CDCl3, menos pura. C13
154.2909
145.3615
137.7306
131.9894
125.9880
77.4737
77.1568
76.8383
34.4480
30.1389
25.0455
18.0397
16.3475
[*1e6]
[ppm]
N
OH
Se
7

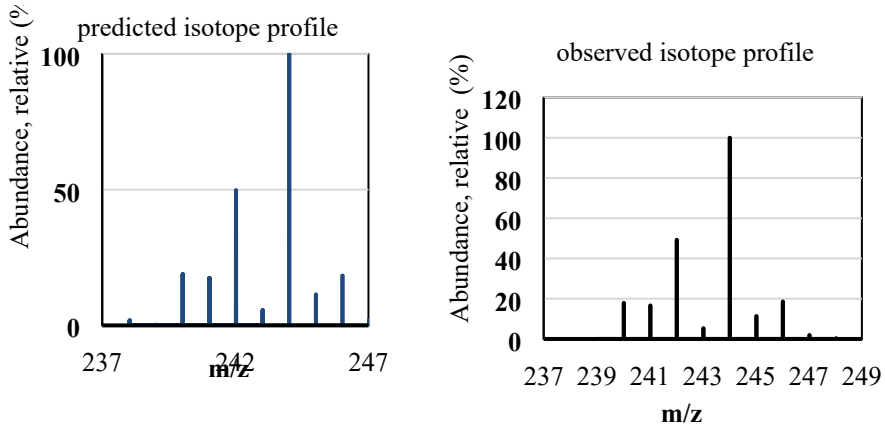
predicted isotope profile
Abundance, relative (%)
100
50
0
237
242
247
m/z
observed isotope profile
Abundance, relative (%)
120
100
80
60
40
20
0
237 239 241 243 245 247 249
m/z

4.8 Lactam 8

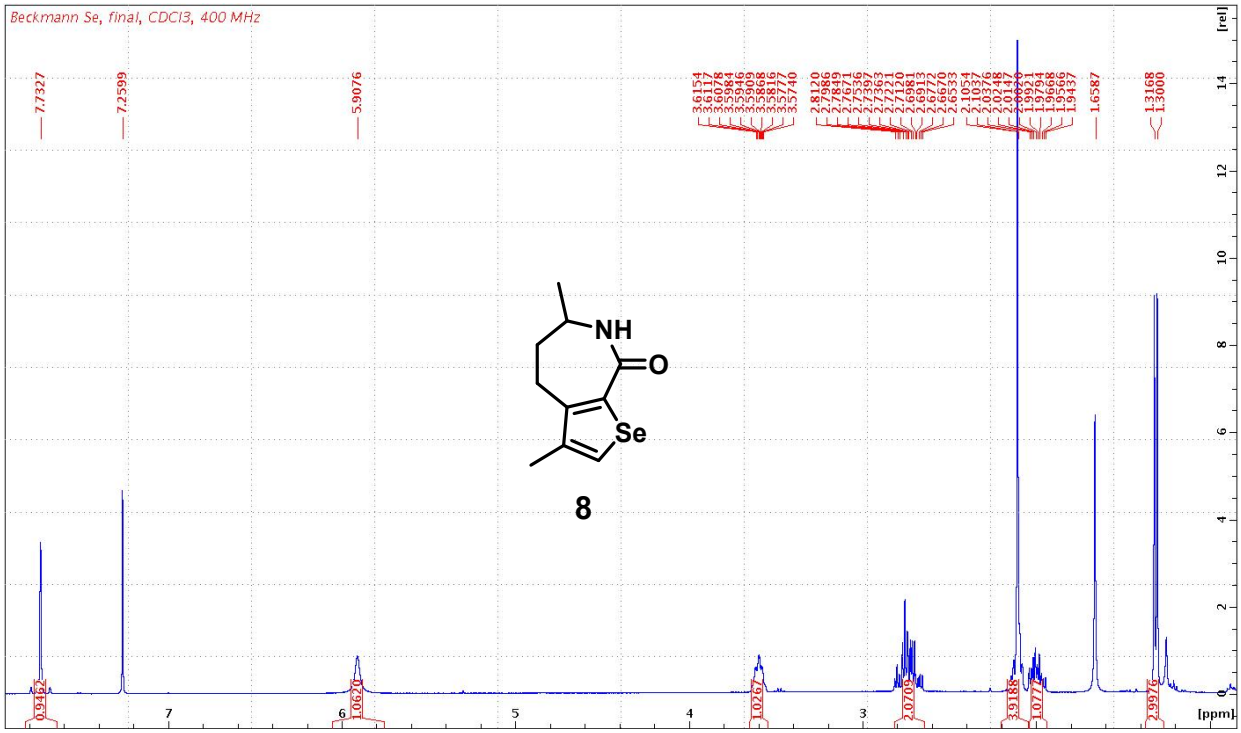
Beckmann Se, final, CDCl3, 400 MHz
7.7327
7.2599
5.9076
1.6587
1.3168
1.3000
NH
O
Se
8
[ppm]
[rel]

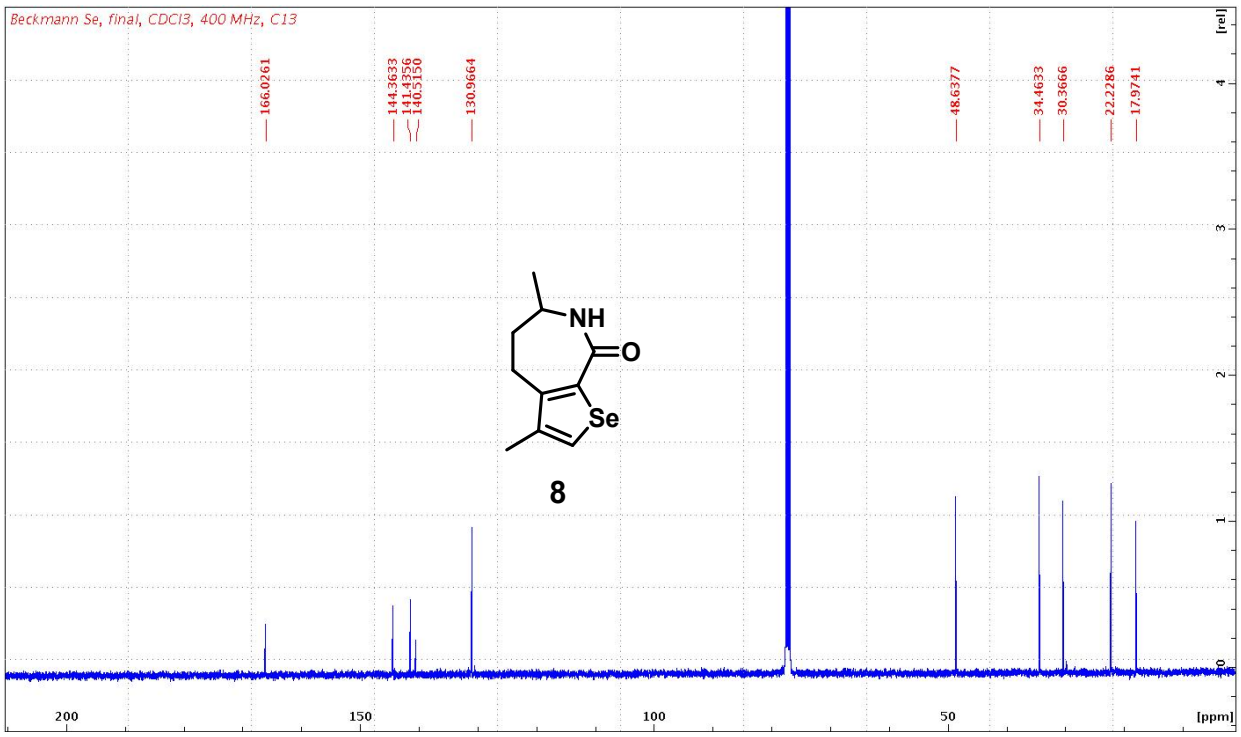
Beckmann Se, final, CDCl3, 400 MHz, C13
166.0261
144.3633
141.4356
140.5150
130.9664
48.6377
34.4633
30.3666
22.2286
17.9741
NH
O
Se
8
[ppm]
[rel]

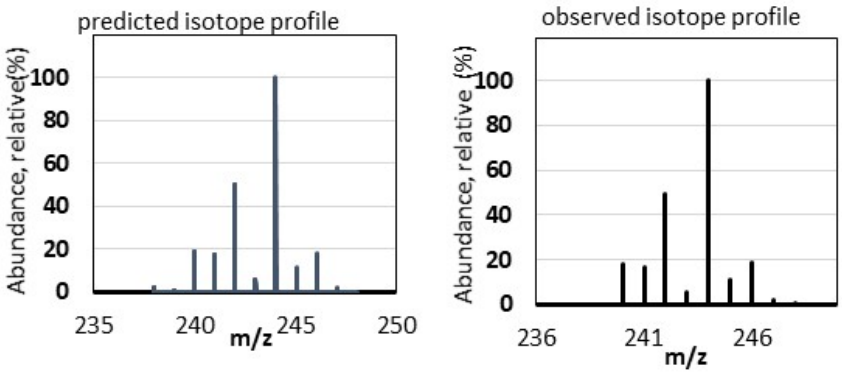
predicted isotope profile
Abundance, relative(%)
m/z
observed isotope profile
Abundance, relative (%)
m/z

[S1] GAUSSIAN 09, Revision **A.01**, M. J. Frisch, G. W. Trucks, H. B. Schlegel, G. E. Scuseria, M. A. Robb, J. R. Cheeseman, G. Scalmani, V. Barone, B. Mennucci, G. A. Petersson, H. Nakatsuji, M. Caricato, X. Li, H. P. Hratchian, A. F. Izmaylov, J. Bloino, G. Zheng, J. L. Sonnenberg, M. Hada, M. Ehara, K. Toyota, R. Fukuda, J. Hasegawa, M. Ishida, T. Nakajima, Y. Honda, O. Kitao, H. Nakai, T. Vreven, J. A. Montgomery, Jr., J. E. Peralta, F. Ogliaro, M. Bearpark, J. J. Heyd, E. Brothers, K. N. Kudin, V. N. Staroverov, R. Kobayashi, J. Normand, K. Raghavachari, A. Rendell, J. C. Burant, S. S. Iyengar, J. Tomasi, M. Cossi, N. Rega, J. M. Millam, M. Klene, J. E. Knox, J. B. Cross, V. Bakken, C. Adamo, J. Jaramillo, R. Gomperts, R. E. Stratmann, O. Yazyev, A. J. Austin, R. Cammi, C. Pomelli, J. W. Ochterski, R. L. Martin, K. Morokuma, V. G. Zakrzewski, G. A. Voth, P. Salvador, J. J. Dannenberg, S. Dapprich, A. D. Daniels, Ö. Farkas, J. B. Foresman, J. V. Ortiz, J. Cioslowski, and D. J. Fox, Gaussian, Inc., Wallingford CT, 2009.

[S2] Hehre, W. J.; Radom, L.; Schleyer, P. v.R.; Pople, J. A. *Ab Initio Molecular Orbital Theory*, John Wiley & Sons, NY, 1986.

[S3] Parr, R. G.; Yang, W. *Density Functional Theory of Atoms and Molecules*; Oxford University Press: New York, 1989.

[S4] (a) J. P. Perdew, K. Burke and M. Ernzerhof, Generalized Gradient Approximation Made Simple *Phys. Rev. Lett.* 1996, **77**, 3865-3868; (b) J. P. Perdew, K. Burke and M. Ernzerhof, Generalized Gradient Approximation Made Simple *Phys. Rev. Lett.* 1997, **78**, 1396-1396. (c) J. P. Perdew, Density-functional approximation for the correlation energy of the inhomogeneous electron gas *Phys. Rev. B* 1986, **33**, 8822-8824.

[S5] (a) R. Ditchfield, W. J. Hehre and J. A. Pople, Self-Consistent Molecular-Orbital Methods. IX. An Extended Gaussian-Type Basis for Molecular-Orbital Studies of Organic Molecules *J. Chem. Phys.* 1971, **54**, 724-728. (b) W. J. Hehre, R. Ditchfield and J. A. Pople, Self-Consistent Molecular Orbital Methods. 12. Further extensions of Gaussian-type basis sets for use in molecular-orbital studies of organic-molecules *J. Chem. Phys.* 1972, **56**, 2257-2261. (c) P. C. Hariharan and J. A. Pople, Accuracy of AH equilibrium geometries by single determinant molecular-orbital theory *Mol. Phys.* 1974, **27**, 209-214. (d) M. S. Gordon, The isomers of silacyclopropane *Chem. Phys. Lett.* 1980, **76**, 163-168. (e) P. C. Hariharan and J. A. Pople, Influence of polarization functions on molecular-orbital hydrogenation energies *Theor. Chim. Acta* 1973, **28**, 213-222.

[S6] (a) C. Peng, P. Y. Ayala, H. B. Schlegel and M. J. Frisch, Using redundant internal coordinates to optimize equilibrium geometries and transition states *J. Comp. Chem.* 1996, **17**, 49-56. (b) C. Peng and H. B. Schlegel, Combining Synchronous Transit and Quasi-Newton Methods for Finding Transition States *Israel J. Chem.* 1993, **33**, 449-454.

[S7] (a) M. T. Cancès, B. Mennucci and J. Tomasi, A new integral equation formalism for the polarizable continuum model: Theoretical background and applications to isotropic and anistropic dielectrics *J. Chem. Phys.* 1997, **107**, 3032-3041. (b) M. Cossi, V. Barone, B. Mennucci and J. Tomasi, Ab initio study of ionic solutions by a polarizable continuum dielectric model *Chem. Phys. Lett.* 1998, **286**, 253-260. (c) B. Mennucci and J. Tomasi, Continuum solvation models: A new approach to the problem of solute's charge distribution and cavity boundaries *J. Chem. Phys.* 1997, **106**, 5151-5158. (d) J. Tomasi, B. Mennucci and R. Cammi, Quantum mechanical continuum solvation models *Chem. Rev.* 2005, **105**, 2999-3094.

[S8] A. V. Marenich, C. J. Cramer and D. G. Truhlar, Universal solvation model based on solute electron density and a continuum model of the solvent defined by the bulk dielectric constant and atomic surface tensions *J. Phys. Chem. B*, 2009, **113**, 6378-6396.

[S9] (a) A. D. McClean and G. S. Chandler, Contracted Gaussian basis sets for molecular calculations. I. Second row atoms, *Z*=11-18 *J. Chem. Phys.* 1980, **72**, 5639-5648. (b) R. Krishnan, J. S. Binkley, R. Seeger and J. A. Pople, Self-consistent molecular orbital methods. XX. A basis set for correlated wave functions *J. Chem. Phys.* 1980, **72**, 650-654. (c) A. J. H. Wachters, Gaussian Basis Set for Molecular Wavefunctions Containing Third-Row Atoms *J. Chem. Phys.* 1970, **52**, 1033-1036. (d) P. J. Hay, Gaussian basis sets for molecular calculations - representation of 3D orbitals in transition-metal atoms *J. Chem. Phys.* 1977, **66**, 4377-4384. (e) K. Raghavachari and G. W. Trucks, Highly correlated systems: Excitation energies of first row transition metals Sc-Cu *J. Chem. Phys.* 1989, **91**, 1062-1065. (f) R. C. Binning Jr. and L. A. Curtiss, Compact contracted basis-sets for 3rd-row atoms - Ga-Kr *J. Comp. Chem.* 1990, **11**, 1206-1216. (g) M. P. McGrath and L. Radom, Extension of Gaussian-1 (G1) theory to bromine-containing molecules *J. Chem. Phys.* 1991, **94**, 511-516. (h) L. A. Curtiss, M. P. McGrath, J.-P. Blaudeau, N. E. Davis, R. C. Binning Jr. and L. Radom, Extension of Gaussian-2 theory to molecules containing third-row atoms Ga-Kr *J. Chem. Phys.* 1995, **103**, 6104-6113. (i) T. Clark, J. Chandrasekhar, G. W. Spitznagel and P. v. R. Schleyer, Efficient diffuse function-augmented basis-sets for anion calculations. 3. The 3-21+G basis set for 1st-row elements, Li-F *J. Comp. Chem.* 1983, **4**, 294-301. (j) M. J. Frisch, J. A. Pople and J. S. Binkley, Self-Consistent Molecular Orbital Methods. 25. Supplementary Functions

for Gaussian Basis Sets *J. Chem. Phys.* 1984, **80**, 3265-3269.

[S10] S. Grimme, J. Antony, S. Ehrlich and H. Krieg, A consistent and accurate ab initio parameterization of density functional dispersion correction (DFT-D) for the 94 elements H-Pu *J. Chem. Phys.* 2010, **132**, 154104.

[S11] (a) A. D. Becke and E. R. Johnson, A density-functional model of the dispersion interaction *J. Chem. Phys.* 2005, **122**, 154101. (b) E. R. Johnson and A. D. Becke, A post-Hartree-Fock model of intermolecular interactions *J. Chem. Phys.* 2005, **123**, 24101. (c) E. R. Johnson and A. D. Becke, A post-Hartree-Fock model of intermolecular interactions: Inclusion of higher-order corrections *J. Chem. Phys.* 2006, **124**, 174104.

[S12] Bruker, "APEX2", Bruker AXS Inc., Madison, Wisconsin, USA, 2009.

[S13] Bruker, "SAINT, Area Detector Control and Integration Software", Bruker AXS, Madison, Wisconsin, USA, 2014.

[S14] Bruker AXS, "SADABS", Bruker Analytical Systems, Madison, Wisconsin, 2014.

[S15] G. M. Sheldrick, "SHELXT - Integrated space-group and crystal-structure determination". *Acta Crystallographica a-Foundation and Advances* 2015, **71**, 3-8, doi:10.1107/s2053273314026370.

[S16] Farrugia, L.J. WinGX suite for small-molecule single-crystal crystallography. 1999, 32, 837-838.

[S17] C.F. Macrae, I.J. Bruno, J.A. Chisholm, P.R. Edgington, P. McCabe, E. Pidcock, L. Rodriguez-Monge, R. Taylor, J. van de Streek, P.A. Wood, *J. Appl. Cryst.*, 2008, **41**, 466-470.

[S18] O.V. Dolomanov, L.J. Bourhis, R.J. Gildea, J.A.K. Howard, H. Puschmann, *J. Appl. Cryst*., 2009, **42**, 339-341.